

The Use of LS-DYNA[®] Models to Predict Containment of Disk Burst Fragments

Eric Stamper¹ and Steven Hale²

CAE Associates Inc.

www.caeai.com

1579 Straits Turnpike, Suite 2B, Middlebury, CT 06762

¹stamper@caeai.com ²hale@caeai.com

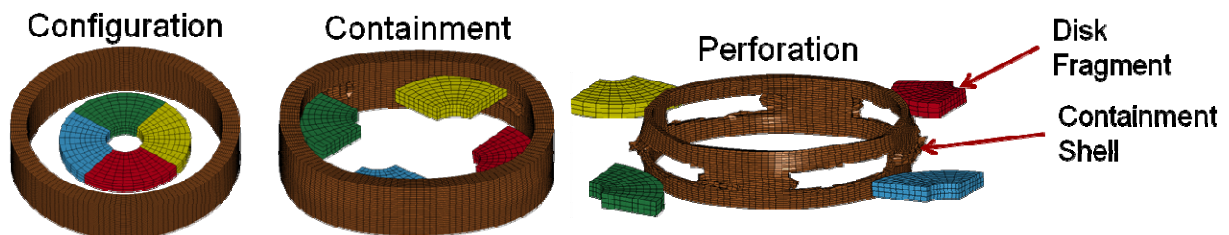
Abstract

Turbomachinery manufacturers commonly test the centrifugal strength of their rotors in a vertical axis spin test, often called a disk burst test. The design of the containment shell that encloses the disk burst event is critical to ensure the safety of the area surrounding the test. A common method used to design the containment shell for a turbine disk burst test is based on the assumption that the kinetic energy lost by the disk fragments during impact is converted into kinetic energy in the containment shell and energy loss to plastic strain and shear failure in the shell. Containment shells are sized such that the energy required to fail the shell material exceeds the kinetic energy loss during impact. This method is approximate because it assumes fully inelastic impacts and does not account for losses due to friction or heat, nor does it account for stress concentrations in the impact zone or complex disk geometries. ANSYS/LS-DYNA was used to develop an analysis method that could provide more accurate predictions of containment failure limits for a wider range of disk and containment geometries. The ANSYS/LS-DYNA models used a piecewise linear plasticity material law with strain rate dependence, segment based eroding contact, nonlocal failure methods, and a consistent element size. Model results showed good correlation with burst test data [1] relative to the prediction of containment, shell perforation, and overall deformation.

Introduction

Turbomachinery manufacturers commonly test the centrifugal strength of their rotors in a vertical axis spin test, often called a disk burst test. The design of the containment shell that encloses the disk burst event is critical to ensure the safety of the area surrounding the test. If the containment shell is not adequately designed, the shell may perforate and release the disk fragment. Burst test designers have a need to predict the minimum dimensions required to contain the burst fragments so they can produce a containment shell that is both safe and cost-effective.

Figure 1: Disk and Containment Shell Geometries Showing the Initial Configuration, Contained State, and Perforated State



Traditionally, the analytical procedures developed by Hagg and Sankey have been used for this purpose [1]. Their equations are based on energy methods and are believed to be limited

to a small range of burst disk and containment shell geometries. In this effort, ANSYS/LS-DYNA models were developed to provide a more reliable tool for predicting containment over a wider range of geometries. Attention was given to supplementing the Hagg and Sankey work by using their published test data to calibrate and compare the results of the ANSYS/LS-DYNA models.

Hagg and Sankey proposed that the containment process was a two stage event, each of which is governed by a unique set of equations. The first stage accounts for localized perforation failure where the fragments perforate the containment shell upon initial impact. The equations assume that perforation failure occurs when the energy transfer during impact as measured by the energy loss of the burst fragment exceeds the maximum compression and shear strain energy that the contact zone of the containment shell is capable of absorbing. The maximum compression and shear strain energies in the shell are based on the compressive flow stress, the failure strain, and the shear strengths of the shell material. The equation used by Hagg and Sankey for energy lost by a fragment in this stage is shown in Equation 1. This equation assumes that the impact is entirely inelastic and there are no losses to friction or heat.

$$(1) \quad \Delta E_{Stage1} = \frac{1}{2} M_1 V_1^2 \left(1 - \frac{M_1}{M_1 + M_2} \right)$$

Where M_1 = Mass of the disk fragment
 V_1 = Velocity of the disk fragment
 M_2 = Effective mass of the shell (part of the shell that responds to the initial contact and momentum transfer).

The criterion for non-perforation is shown in Equation 2.

$$(2) \quad E_s + E_c > \Delta E_{Stage1}$$

Where E_s = Maximum shear strain energy of an effective volume
 E_c = Maximum compressive strain energy of an effective volume

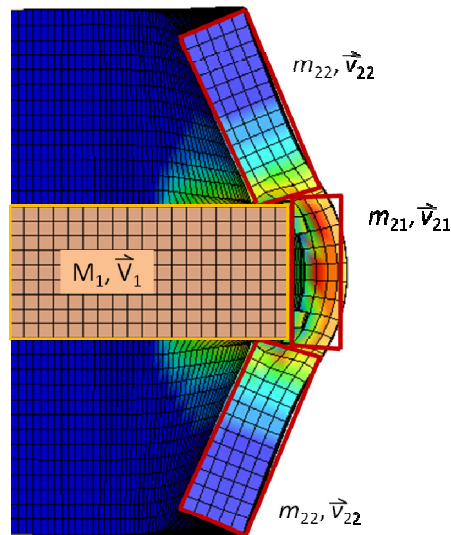
The effective mass (M_2) in Equation 1 is based on the volume in the shell adjacent to the impact zone (with a mass of m_{21}) and volumes both above and below this zone (with masses of m_{22} each) as shown in Figure 2. Combining Equation 2 with Equation 1 and using additional terms for effective mass yields Equation 3 for non-perforation.

$$(3) \quad E_s + E_c > \frac{1}{2} M_1 V_1^2 - \frac{1}{2} (M_1 + m_{21}) v_{21}^2 - \frac{1}{2} m_{22} v_{22}^2$$

Where v_{21} = the maximum velocity of mass m_{21} after impact (residual velocity)
 v_{22} = the maximum velocity of mass m_{22} after impact (residual velocity)

If localized perforation failure does not occur, the process moves to the second stage. In this stage, the residual energy is dissipated in the form of tensile strain throughout an extended volume of the shell material. Failure occurs when the remaining energy exceeds the allowable strain energy in this extended volume.

Figure 2: Shell Volumes Used in the Calculation of Effective Mass and Residual Velocity



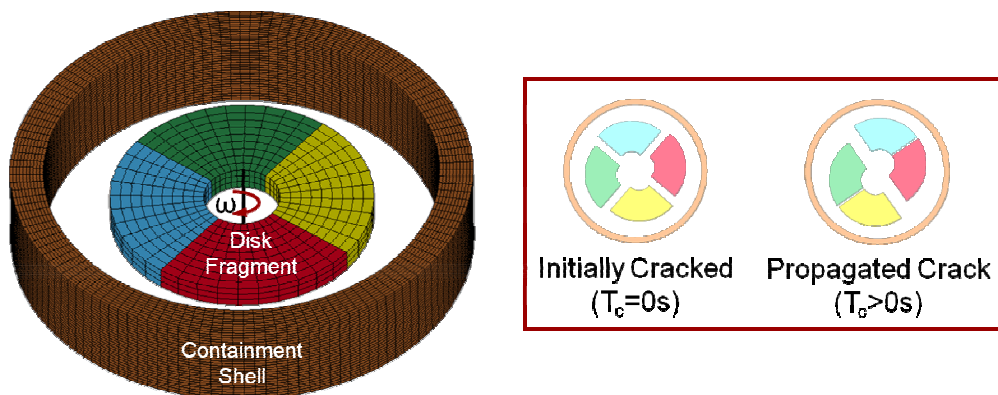
The above equations include a number of assumptions that call into question the accuracy of this method for predicting failure in the containment shell. Specifically, it assumes perfectly inelastic deformation upon impact which does not account for energy stored as elastic strain, nor does it account for losses to friction or heat. In addition, the equations for effective mass and post-impact velocity in the shell are only approximations. Another approximation of this method is that it is entirely based on energy and momentum transfer on a macro-mechanics level and, as such, it does not account for local stress concentrations in the contact zone.

Hagg and Sankey showed good agreement between their analytical predictions of failure and their test results, particularly in Stage 1. However, the applicability of their methods to a wide range of disk and shell shapes and sizes, to different materials, and to containment of other rotating structures is questionable due to the numerous approximations and simplifications. The ANSYS/LS-DYNA models were developed as a possible means of eliminating many of these simplifications.

Model Setup

The disks used in the test series were notched at four quadrants on the inner diameter which forced them to crack into four equal fragments. The ANSYS/LS-DYNA models were constructed with four initially separate and symmetric disk segments, each with an angular velocity (ω) applied as shown in Figure 3.

Figure 3: Initial Model Configuration



Hagg and Sankey noted that cracking in the disks would occur in steps that first caused them to separate in half and secondly into quarters. In the models, crack propagation was simplified by assuming that the crack propagation time (T_c) was zero, causing four equal disk fragments to separate from each other at the start of the analysis. This assumption resulted in all four fragments concurrently impacting the containment shell.

Material Modeling

The materials used in the tests were 33Cr-48Mo-8V-11-Fe forged alloy for the disk and a low-carbon, hot rolled ASTM A283 grade C steel for the containment shell. The disk was modeled as a rigid body to simplify the model and speed up run times. This assumption was made based on the test data which showed little relative deformation and no additional fragmentation in the disk fragments following impact. Furthermore, the dissimilar material strengths between the disk and containment shell suggested that this would not significantly affect the accuracy of the models. Also, the assumption is conservative with respect to containment since all plastic work occurs in the containment shell.

The shell was made from a low-carbon, hot rolled ASTM A283 grade C steel with the properties listed in Table 1.

Table 1: Shell Material Properties for Tests:1-10 at Strain Rates = $0s^{-1}$

Experiment	Young's Modulus [psi]	Density [lb_m/in^3]	Poissons Ratio
All	30E+06	0.284	0.3

	Yield Strength [psi]	Ultimate Strength [psi]	Failure Strain*
Test 1	40,444	50,000	0.584
Test 2	51,111	62,000	0.680
Test 3	54,489	65,800	0.710
Test 4	54,489	65,800	0.710
Test 5	51,111	62,000	0.680
Test 6	54,311	65,600	0.709
Test 7	57,156	68,800	0.734
Test 8	54,844	66,200	0.714
Test 9	59,556	71,500	0.756

*Interpolated values based upon ultimate strength material ranges

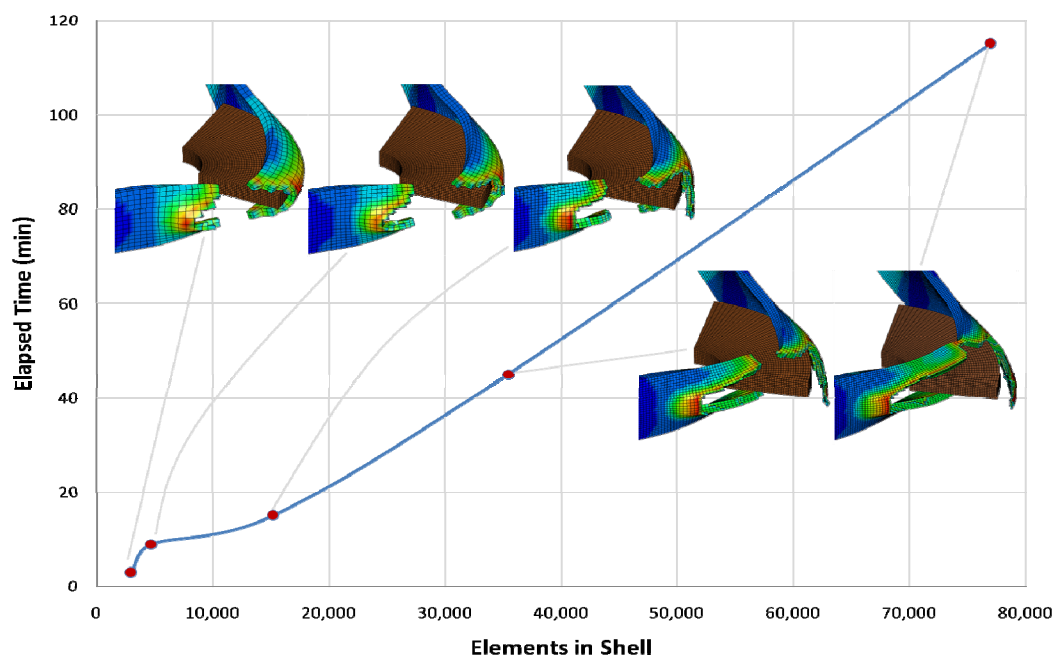
The values shown are based on material testing that was performed on each lot of material used to create the containment shell. The published data only provided ultimate strength values which were then interpolated to determine corresponding yield strengths and failure strains (within the provided ranges for all of the tests).

Strain-rate hardening was also included for the shell material to extend the range of applicability to the high strain-rates in the impact zone. It was assumed that the tangent modulus, yield stress, and ultimate strength of the material would have a similar dependence on strain rate as a similar material described in the work of Dietenberger, Buyuk, and Kan [2]. These properties were incorporated into the model in the form of a piecewise-linear plasticity model where the true stress vs effective plastic strain curves were input for given strain rates.

Mesh Density Considerations

It is well known that mesh density is a prime consideration in the determination of model accuracy and simulation time. The accuracy of the solution can increase with a higher local mesh density in the regions of high stress gradients such as the contact zone. However, this usually results in longer run times. Furthermore, it is well documented that there is an element size dependency inherent to models that include failure due to damage growth [3,4]. Therefore, a mesh density study was performed to determine when the effects of failure remained constant with an increase in element count for a uniform distribution of elements in the shell. Details of this study are shown in Figure 4 where simulation (elapsed) time is also plotted. It was found that the failure mode and deformation pattern remained relatively constant from about 18,000 to 35,000 elements. A final size of 35,000 elements was selected for this geometry because it was deemed to provide a good compromise between accuracy and simulation time.

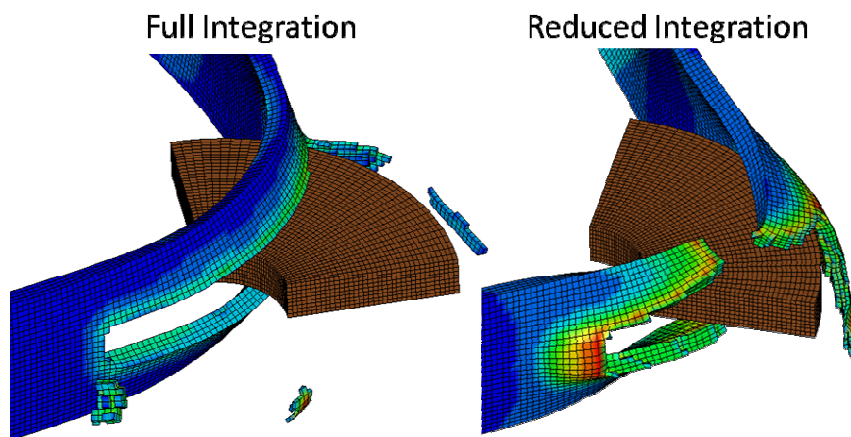
Figure 4: Failure Deformation and Simulation Time Vs. Mesh Size



Element Formulation Considerations

The shape and formulation of the solid elements were also considered in this study as they contribute to the accuracy of the failure prediction and the total simulation time. All of the elements used in the analysis were 8-node linear hexahedral solids with single point, reduced-integration. The reduced-integration formulation was used to improve the accuracy of the element bending and shearing prediction because, unlike full-integration elements, they are not susceptible to shear locking. The impact and failure behavior of shells with both full and reduced integration elements is shown in Figure 5. Notice that the fully-integrated elements show a stiffer, more brittle response as compared to the relatively ductile response in the reduced-integration elements.

Figure 5: Failure Deformation for Shell Models with Full and Reduced Integration Elements

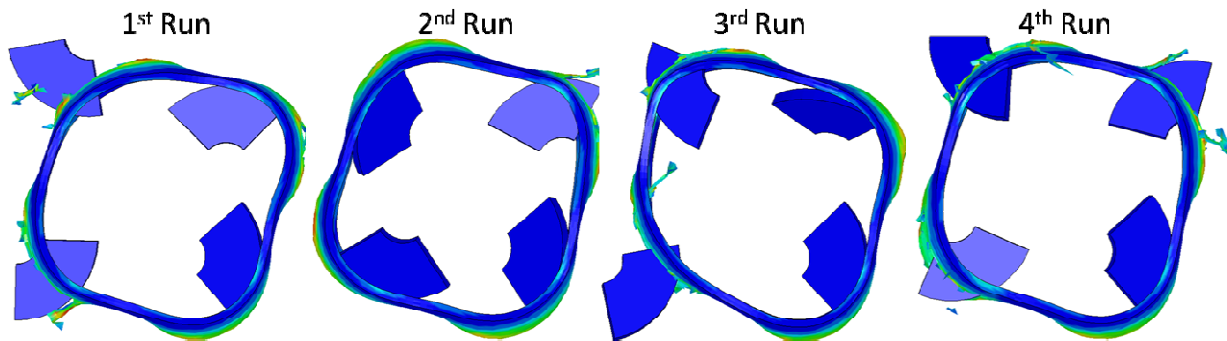


Hourglass control was added to the models to minimize hourglass deformations that can occur in reduced-integration elements. In this case, the LS-DYNA viscous-based hourglass control type 3 (Flanagan-Belytschko form with exact volume integration) was used with an hourglass coefficient of 0.01 [5]. The hourglass coefficient was lowered to 0.01 from the default of 0.1 to minimize the potential for artificially damping the kinetic energy of the system.

Asymmetric Results

During the course of this study it was discovered that inconsistent and asymmetric results can occur for models that include element failure even when no changes are made to the model, software, or hardware. Specifically, the inclusion of element failure and subsequent erosion lead to asymmetric results despite the use of symmetry in the mesh, boundary conditions, and impact loads. The asymmetric failure response of four different runs with the same model is illustrated in Figure 6. All of these runs used the exact same model executed on the same computer with the same version of LS-DYNA and only one processor. The failure behavior changed significantly with each successive run to the point where the model could not be used to reliably predict containment. Some of this inconsistency was reduced by using the double-precision version of LS-DYNA with consistency checking, but the problem remained.

Figure 6: Failure Response of Four Identical Models



Non-Local Failure Method

The non-local failure method included in LS-DYNA (*MAT_NONLOCAL) was used to overcome the asymmetric failure response described in the previous section. This method is primarily used to mitigate the size-dependency of damage and failure in finite elements. According to the work of Deslauriers, Cronin, and Duquette, damage-based models have an inherent element size dependency [3]. To mitigate this behavior, a nonlocal damage function can be used which distributes the material damage over a representative volume of material. Additional work by Feucht, Sun, Erhart, and Frank (2006) showed a strong dependency on element size of the damage parameters used in the Gurson and Wilkins damage models [4].

In this study, the *MAT_NONLOCAL command in LS-DYNA was used to include the nonlocal algorithm as described in the LS-DYNA Keyword User's Manual (Version 971) [5]. The plastic strain was used as the damage function for which the nonlocal method was applied. This algorithm uses a weighting function to average damage values over a volume surrounding each element. It effectively increases damage in elements with neighboring elements that have more damage and decreases damage in elements with neighbors that have less damage. These models used P and Q exponents of 8 and 2 respectively, and a characteristic length equal to 3 times the average element length. This causes the plastic strain to average over a radius encompassing 3 elements on all sides. Once this method was implemented, very consistent and symmetric failure patterns were observed for models having the same geometry, loads, and material properties.

Other Model Inputs

Contact: The contact method used in the models was LS-DYNA Eroding Surface-to-Surface contact with the SOFT field set to 2. This implements segment-based contact which was shown to reduce simulation times by approximately 35% for these models without affecting failure prediction.

Friction: The friction coefficient was fixed at 0.2 for all models. Only static friction was used.

Element size: A constant element size of 0.25 inches per element edge length was used in the containment shells of all models based on the earlier mesh density study. The element sizes in all disk fragments was also fixed. While this causes a variation in mesh density with changes in disk size, it also provides a constant ratio of element sizes between the disk fragment and the shell, and provides for a consistent set of parameters in the *MAT_NONLOCAL model.

Results

A total of ten individual tests were performed each with varying material properties, test geometries, and spin loads. The main objective of the analysis was to correlate the prediction of shell perforation to the test data. The average tensile elongation in the containment shell and the overall deformed shape were additional metrics used in the correlation. The table below lists the results for both the test (ASME [1]), the analysis (LS-DYNA), and their correlation for each of the ten test configurations. The failure modes listed in the table include containment, perforation, and tension. Perforation failure refers to first stage penetration failure as described in the paper by Hagg and Sankey while tension failure refers to second stage failure in which tensile strain induced in a larger volume of shell generates a complete tensile crack through the entire section of the shell.

Table 2: Model Correlation to Test Data

	ASME Results		LS-Dyna Results		Correlation
	Failure	Tension ϵ (%)	Failure	Tension ϵ (%)	Failure Mode
Test1	Perforation	X	Perforation	X	Yes
Test2	Containment	4.6	Containment	2.7	Yes
Test3	Containment	6.9	Containment	4.7	Yes
Test4	Containment	11	Containment	7.8	Yes
Test5	Perforation	X	Perforation	X	Yes
Test6	Tension	10	Containment	9.1	1*
Test7	Tension	6.0	Containment	9.5	2*
Test8	Containment	12	Containment	13.2	Yes
Test9	Containment	6.5	Containment	6.7	Yes
Test10	Tension	3.6	Containment	3.8	3*

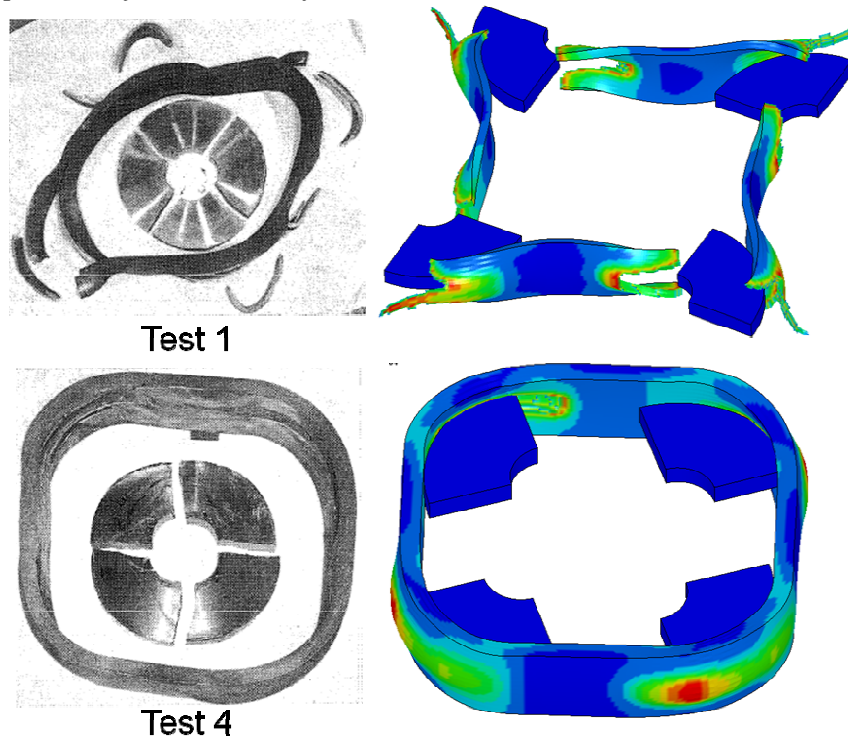
1* Weld defect in test caused tension failure without perforation. Analysis predicted perforation failure only.

2* Test contained disk but had a tension failure, Analysis predicted containment only.

3* Test showed the fragment rupturing the containment shell, which the analysis did not predict. Both contained fragment.

Overall, the models provide a good correlation to the failure modes recorded in the tests. However, the second stage tension failure modes were not predicted by the models. Hagg and Sankey reported that, for Test 6 at least, there was a noticeable defect in the single weld seam in the disk which also happens to be where the tensile failure occurs. It is theorized that weakness in the weld region may cause the three tension failure modes observed in the tests.

A qualitative comparison of the overall final deformations in the shell is shown in Figure 8 for the subset of tests that included photographs [1].

Figure 8: Comparison of the Final Deformed Geometries

Conclusions

The energy equations proposed by Hagg and Sankey have traditionally been used to design containment shells for disk burst tests. However, it is believed that these methods are restricted to a limited range of disk and shell geometries because of the many simplifications used in their development. ANSYS/LS-DYNA was used in this study as an alternate tool for designing containment structures. The ANSYS/LS-DYNA models successfully predicted disk burst containment, demonstrating their potential as a reliable tool for containment design. It is believed that the methods developed in this study can be applied to more complex disk and containment geometries as well as containment designs for other rotating structures. This study also demonstrated the use of nonlocal failure methods to significantly improve the reliability and symmetry of results that depend on damage and failure.

References

- [1] Hagg, A.C and Sankey, G.O., "The containment of Disk Burst Fragments by Cylindrical Shells," ASME Paper No.73-WA-Pwr-2, 1973.
- [2] Dietenberger, M., Buyuk, M. and Kan, C., "Development of a High Strain-Rate Dependent Vehicle Model" 4th German LS-DYNA Forum, Bamberg, Germany, 2005.
- [3] Deslauriers, P., Cronin, D., and Duquette, A., "Numerical Modeling of Woven Carbon Composite Failure", 8th International LS-Dyna Users Conference, 11-33, Dearborn, MI, 2004.
- [4] Feucht, M., Sun, D.Z., Erhart, T., and Frank, T. "Recent Development and Applications of the Gurson Model", 5th German LS-DYNA Forum, Ulm, Germany, 2006.
- [5] Livermore Software Technology Corporation, "LS-Dyna Keyword User's Manual", Version 971, May 2007.

